European Journal of Mechanics A/Solids 53 (2015) 282–293

Contents lists available at ScienceDirect

European Journal of Mechanics A/Solids

journal homepage: www.elsevier.com/locate/ejmsol

A microstructurally-based internal length for strain localization problems in dynamics

Bertrand François [a, *], Oumar Keita [b]

[a] Building Architecture and Town Planning Department (BATir), Université Libre de Bruxelles (ULB), Avenue F.D. Roosevelt, 50 – CPI 194/2, 1050 Bruxelles, Belgium
[b] Laboratoire CRISMAT/ENSICAEN/UCBN/CNRS, UMR 6508, 6 Bd du Maréchal Juin, 14050 Caen, France

ARTICLE INFO

Article history:
Received 28 October 2014
Accepted 21 May 2015
Available online 30 May 2015

Keywords:
Damage
Strain localization
Internal length

ABSTRACT

Classical finite element method including strain-softening materials suffers from a mesh-dependency solution. The thickness of the bands in which strains are localized is arbitrarily narrow and may lead to a rupture without energy consumption. This is the case in quasi-static as well as in dynamics problems. The present paper uses a two-scale dynamic damage law that is based on an intrinsic length at micro-scale, corresponding to the inter-distance between two adjacent micro-cracks, that regularizes the strain localization problem in dynamics. The material response is time-dependent due to the inertial effect of the micro-crack propagation. This produces a natural, microstructurally-based, delayed response of the material that, in turn, removes the mesh-sensitivity in dynamics. As a consequence, the size of the strain localization band is controlled by the internal length of the material.

1. Introduction

1.1. Softening, strain localization and regularization

Quasi-brittle materials exhibit strain softening when they are loaded beyond their ultimate strength. The post-peak stress-strain response of the material is characterized by a decreasing secant stiffness and a negative tangent stiffness. When materials experience strain softening, the governing incremental equilibrium equations lose ellipticity under quasi-static conditions (Bazant, 1976; Peerlings et al., 2002; Sulem, 2010; Nicot and Darve, 2011); while under dynamic conditions, the wave speed become imaginary (Hill, 1962; Lasry and Belytschko, 1988). From a physical point of view, the vanishing stiffness in a given region implies that the wave speed reduces to zero in that region leading to the phenomenon of "wave trapping" as discussed in Wu and Freund (1984). Actually, the wave remains trapped in the first element where the stiffness vanishes and the strain accumulates in that element.

As a consequence, conventional boundary value problems are ill-posed and the solution is pathologically mesh-dependent. The material exhibits a localized rupture on a thickness which is undetermined. In finite element computations, the thickness of the localized band becomes a function of the mesh size. One of the consequences is that the localized deformation can become arbitrarily narrow and the rupture can occur without energy consumption which is physically non-admissible (Bazant and Pijaudier-Cabot, 1998).

A series of regularization techniques have been developed to overcome this pathological mesh sensitivity. Most of them consist in the introduction of a characteristic length that controls, directly or indirectly, the thickness of the localized band (see De Borst et al. (1993) for extensive review and benchmarking of those methods).

(i) In non-local approaches, a variable that controls the behaviour of the material in one point is obtained as a function of the material state not only at that point but also in a given surrounding zone. The distance between the considered point and the border of the zone introduces intrinsically an internal length (Bazant et al., 1984; Belytschko et al., 1986; Pijaudier-Cabot and Bazant, 1987; Bazant, 2002).
(ii) Enhanced-gradient constitutive models use a strain definition which is not limited to the first order but takes also into account higher orders of the Taylor series. The coefficients of the Taylor's development depend on an internal length (Peerlings et al., 1996; Sluys et al., 1993). Actually, gradient-dependent models can be derived from the framework of

* Corresponding author.
E-mail address: bertrand.francois@ulb.ac.be (B. François).

http://dx.doi.org/10.1016/j.euromechsol.2015.05.012
0997-7538/

non-local approaches, as demonstrated by Mühlhaus and Aifantis (1991).

(iii) Local second gradient formulation consists in the enrichment of the balance equilibrium equation in the framework of microstructure continuum theory (Aifantis, 1984), in which a microkinematic gradient field is introduced to describe strain and rotation at the microscale. The higher-order stress tensor is related to the second gradient tensor toward a constitutive relation depending on an internal length (Mindlin, 1965; Mühlhaus, 1989; De Borst and Sluys, 1991; Chambon et al., 2001; Collin et al., 2006).

Those regularization techniques have the merits to eliminate the mesh dependence pathology but the introduced internal length has rarely a physical meaning. From a conceptual point of view, the internal length should be a material parameter function of the characteristic length of its microstructural features, but in practice it is, most of the time, a phenomenological parameter that is added to make the mathematical problem well-posed and to obtain a realistic thickness of localized band.

(iv) Finally, a last family of regularization techniques consists in introducing a rate-dependence in the stress-strain behavior of materials. Needleman (1988) demonstrates that, when rate-dependence is accounted for, there is no loss of ellipticity in quasi-static conditions and the wave speed remains real in dynamic problems. Actually, the material rate dependence, when combined with strain rate gradient, implicitly introduces a length scale into the boundary value problem formulation. Upon static loading, strain rate gradient comes from the heterogeneity of the strain field. Additionally, upon dynamic conditions, the wave propagation induces also a temporary strain rate gradient.

This last way to regularize a boundary value problem for strain softening materials may appear to be more physical if the material exhibits a "natural" time-dependent behavior. Otherwise, if the delayed response is artificially introduced in the constitutive law only for a regularization purpose, the physical meaning is also lost.

Most of the time, this delay effect in the material behavior is incorporated through phenomenological models (Desmorat et al., 2010; Sluys and De Borst, 1992; Wang et al., 1996; Glema et al., 2000; Graff et al., 2004; Pedersen et al., 2008). Those different models permit a regularization of the strain localization problem. However, for dynamics problem, the determination of the phenomenological parameters that control the rate dependency is not an easy task, due to very short period of time upon which the processes take place. Consequently, time-dependent phenomenological models in dynamics remains relatively delicate because of the lack of data for the parameters calibration. This limitation may justify the use of a micromechanically-based model in which the physics is based on quantifiable mechanisms at fine scale. On the other hand, the micro-mechanically based models require having sufficient data to quantify the physics at that scale, and in particular to know the size of the microstructure. If not, the constitutive parameters of the model can still be obtained by calibration to fit the macroscopic response, even if this is not the primary way to fix the parameters.

1.2. Damage of quasi-brittle material in dynamics

In quasi-brittle materials (such as rock, concrete, ceramics or hard soil), the loss of stiffness is known to be sensitive to internal fractures which are commonly characterized as damage. Damage evolution induces a softening behavior of the material due to a progressive decrease of the material stiffness until zero when micro-cracks coalesce, leading to macro-cracking.

The effects of damage are especially important in phenomena that involve high and rapid changes of stress level. At high loading rates the evolution of damage is sensitive not only to the initial damage, but also to the rate at which the load is applied. The rate of damage evolution and the rate of loading can be of the same order of magnitude, even for very brittle materials. Consequently, inertial effects are of primary importance and brittle materials upon quasi-static loadings may appear to be relatively ductile when they are loaded upon high strain rates.

As already mentioned, phenomenological models suffer from the difficulty to calibrate parameters under such fast processes. An alternative could be, when sufficient information at micro-scale are available, to address this issue from the analysis of micro-structural damage processes for which the mechanics of micro-cracks and their overall response to applied loading must be considered.

Several micro-mechanic-based models have been developed to study damage process under dynamic compressive response of brittle solids such as: the cylindrical model of pore (Zhang et al., 1990); the model of collision of dislocation (Wong, 1990); and the sliding crack model, developed originally by Brace and Bombolakis (1963) and used more recently by many authors, for quasi-static problem (Nemat-Nasser and Horii, 1982; Ashby and Hallam, 1986; Wang and Shrive, 1995) or dynamic problem (Nemat-Nasser and Deng, 1994; Ravichandran and Subhash, 1995; Huang, 2002; Bhatt et al., 2011). The macroscopic damage evolution is due to micro-cracks propagation that takes place at micro-scale. At that scale, the damage mechanism occurs in mode I (tension), even if the macroscopic loading is in compression.

Recently, Keita et al. (2014) developed a continuum damage model accounting for inertial effects deduced from a two-scale framework analysis. The asymptotic homogenization of the small-scale description of dynamic micro-cracks propagation under tensile loading (mode I) leads to a macroscopic damage model in which the rate dependency effect is controlled by the combination of the speed of micro-crack propagation and the size of the microstructure, which is a micromechanically-based internal length.

1.3. Purpose of this study

The purpose of this paper is to show that the consideration of a micro-cracked material with a natural internal length (related to the periodic distribution of micro-cracks), when homogenized, leads to a time-dependent dynamic damage behaviour which, in turn, regularizes the dynamic boundary value problem formulation. The rate dependence does not follow from a phenomenological assumption but is the consequence of the homogenization procedure that considers, by essence, an internal length that is micromechanically-inspired. Actually, this macroscopic dynamic damage model, developped by the same authors in a previous paper (Keita et al., 2014), including a microstructurally-based internal length, can be seen as an enhanced model that unifies the regularization techniques based on the introduction of an internal length and the ones considering a rate-dependent response.

The paper is structured as follows. First the macroscopic damage model deduced from the considerations of dynamic crack propagation at micro-scale is briefly recalled. The focus is particularly made on the key role of the internal length, that is a consequence of the asymptotic homogenization procedure and that will control the thickness of the strain localization band in dynamics. Typical stress-strain responses are presented on uniaxial tensile tests in order to illustrate the brittle–ductile transition controlled by the rate of loading and the internal length. Then, a simple one-dimensional

boundary value problem in dynamics is presented. Finally, this problem is solved under specific conditions that generate strain localization in a part of the bar in order to show the ability of the model to eliminate the pathological mesh sensitivity.

2. Micromechanically-based damage model in dynamics

The model is constructed from an asymptotic homogenization procedure in two stages. First, the stress–strain relationship for a non-evolving microstructure is obtained according to the classical asymptotic developments originally proposed by Benssousan et al. (1978) and Sanchez-Palencia (1980). The output of this first homogenization procedure is the homogenized elastic tensor for a given damage value. Secondly, the damage evolution law is deduced from a micro-mechanical energy analysis that is upscaled according to the asymptotic homogenization scheme. The model development has been extensively detailed in Keita et al. (2014). The present work uses the model previously developed. However, the purpose here is to focus on the role of this model in the regularization of the strain localization problem, which was not discussed in Keita et al. (2014). So, the model has been implemented in a finite element code to treat boundary value problems, taking into account dynamic phenomena through the inertial effect at macro-scale (i.e. wave propagation and wave reflection on the boundaries). For the sake of clarity, this section summarizes the equations and the principles of the model previously developed.

2.1. A microstructurally-based internal length

In this two-scale approach, the microstructure of the material is idealized by a squared representative element containing one centered straight vertical micro-crack. This element is periodically distributed in the material, at least locally. The size of the element ε is the internal length of the problem. From a physical point of view, it is the size of the microstructure which is, in this simplified geometry, the inter-distance between the centers of two neighbor micro-cracks (assumed periodically distributed). The length of each micro-crack is l (Fig. 1a). In this context, the definition of the damage variable d is relatively simple. d is the ratio between the micro-crack length and the cell size:

$$d = \frac{l}{\varepsilon} \tag{1}$$

The damage variable varies between 0 (for intact material) and 1 (for complete damaged material). When $d = 1$, adjacent micro-cracks coalesce leading to a macro-crack unable to transmit tensile stress. Consequently, for $d = 1$, the normal stiffness in tensile mode vanishes to zero.

The constant periodicity of the material is an assumption of the model. However, in a boundary value problem, as addressed below, this periodic condition must be fulfilled locally. The crack length (i.e. the damage variable) may vary smoothly in the material, leading to possible localized damage. In the fully damaged zone, all the micro-cracks are fully developed and coalesce into a macro-crack, while out of that zone, micro-cracks remain essentially inactivated.

2.2. Homogenized stress–strain relationship

The objective of this first step of the homogenization procedure is to deduce the stress–strain relationship for a given microstructure. Assuming the simplified geometry described in Fig. 1a, the material matrix is assumed to behave as a two-dimensional isotropic elastic medium:

$$\sigma_{ij}^{\varepsilon} = a_{ijkl} e_{xkl}(\mathbf{u}^{\varepsilon}), \tag{2}$$

where a_{ijkl} is the elasticity tensor. $\sigma_{ij}^{\varepsilon}$ is the stress field and $\mathbf{u}^{\varepsilon}$ the displacement field from which the strain tensor is deduced in the small deformation hypothesis

$$e_{xij}(\mathbf{u}^{\varepsilon}) = \frac{1}{2}\left(\frac{\partial u_i^{\varepsilon}}{\partial x_j} + \frac{\partial u_j^{\varepsilon}}{\partial x_i}\right). \tag{3}$$

We consider the instantaneous equilibrium of the initial heterogeneous medium in a dynamic context. The momentum equilibrium is

$$\frac{\partial \sigma_{ij}^{\varepsilon}}{\partial x_j} = \rho \frac{\partial^2 u_i^{\varepsilon}}{\partial t^2} \tag{4}$$

where ρ is the mass density of the solid matrix and t is the time.

On the crack faces, traction free conditions are assumed:

$$\boldsymbol{\sigma}^{\varepsilon}\mathbf{N} = 0 \tag{5}$$

where $\mathbf{N}$ is a unit normal vector on the crack faces.

For the homogenization purpose, a reference unit cell Y referred to microscopic coordinates (y_1,y_2) is obtained by rescaling the periodic cell with the internal length ε (Fig. 1b). We assume that the microstructural length ε is small enough with respect to the characteristic dimensions of the whole body, so that to distinguish between microscopic and macroscopic variations. These variations

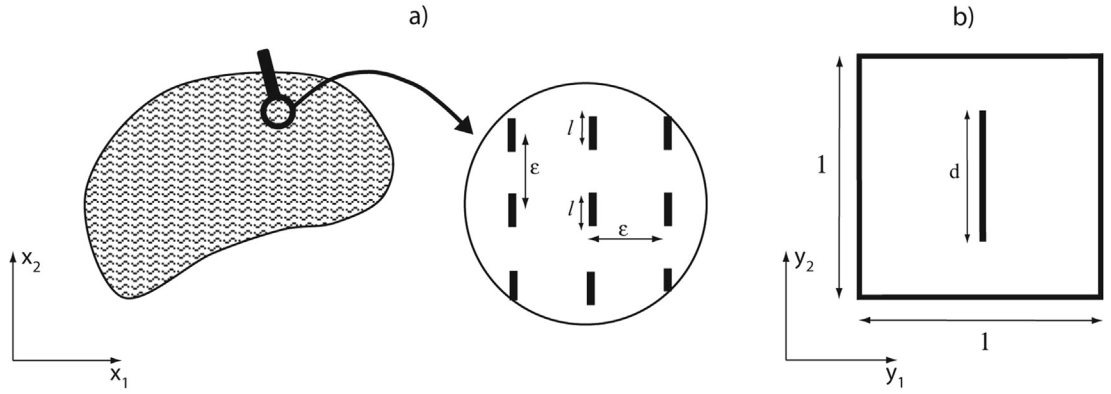

Fig. 1. (a) Micro-fissured medium with locally periodic microstructure, ε is the size of a period and l is the local micro-crack length. (*b*) Unit cell with rescaled crack of length d.

of mechanical fields at different scales are represented by distinct variables: $\mathbf{x}$ the macroscopic variable and $\mathbf{y}=\mathbf{x}/\varepsilon$ the microscopic variable (Fig. 2). For a variable depending on both x and y the total spatial derivative takes the form

$$\frac{d}{dx_i}=\frac{\partial}{\partial x_i}+\frac{1}{\varepsilon}\frac{\partial}{\partial y_i} \tag{6}$$

Following the method of asymptotic homogenization (e.g. Bensoussan et al. (1978); Sanchez-Palencia (1980)), we look for expansions of $\mathbf{u}^\varepsilon$ and $\boldsymbol{\sigma}^\varepsilon$ in the form

$$\mathbf{u}^\varepsilon(\mathbf{x},t)=\mathbf{u}^{(0)}(\mathbf{x},\mathbf{y},t)+\varepsilon\mathbf{u}^{(1)}(\mathbf{x},\mathbf{y},t)+\varepsilon^2\mathbf{u}^{(2)}(\mathbf{x},\mathbf{y},t)+\ldots \tag{7}$$

$$\boldsymbol{\sigma}^\varepsilon(\mathbf{x},t)=\frac{1}{\varepsilon}\boldsymbol{\sigma}^{(-1)}(\mathbf{x},\mathbf{y},t)+\boldsymbol{\sigma}^{(0)}(\mathbf{x},\mathbf{y},t)+\varepsilon\boldsymbol{\sigma}^{(1)}(\mathbf{x},\mathbf{y},t)+\ldots \tag{8}$$

where $\mathbf{u}^{(i)}(\mathbf{x},\mathbf{y},t),\boldsymbol{\sigma}^{(i)}(\mathbf{x},\mathbf{y},t),\quad \mathbf{x}\in\mathscr{B},\quad \mathbf{y}\in Y$ are smooth functions and Y-periodic in $\mathbf{y}$.

The y-dependence of the mass density and the stiffness tensor is assumed:

$$\rho^\varepsilon(\boldsymbol{x})=\rho(\boldsymbol{y})=\rho\left(\frac{\boldsymbol{x}}{\varepsilon}\right) \tag{9}$$

$$a^\varepsilon_{ijkl}(\boldsymbol{x})=a_{ijkl}(\boldsymbol{y})=a_{ijkl}\left(\frac{\boldsymbol{x}}{\varepsilon}\right) \tag{10}$$

The functions $\rho(\boldsymbol{y})$ and $a_{ijkl}(\boldsymbol{y})$ are supposed to be Y periodic.

The fundamental method of asymptotic homogenization consists in substituting the asymptotic development of $\boldsymbol{\sigma}^\varepsilon$ and $\mathbf{u}^\varepsilon$ (Eqs. (7) and (8)) into the elasto-dynamic Eqs. (2)–(4) and taking into account the relation (6). It leads to the followings expressions

$$\frac{\partial\sigma^{(I)}_{ij}}{\partial x_j}+\frac{\partial\sigma^{(I+1)}_{ij}}{\partial y_j}=\rho\frac{\partial^2u^{(I)}_i}{\partial t^2} \tag{11}$$

$$\sigma^{(I)}_{ij}=a_{ijkl}\left(e_{xkl}\left(\mathbf{u}^{(I)}\right)+e_{ykl}\left(\mathbf{u}^{(I+1)}\right)\right) \tag{12}$$

Finally, those equations can be solved for each order I. Doing so, one can demonstrate that the homogenized problem is controlled by the following homogenized momentum balance equation:

$$\frac{\partial}{\partial x_j}\left\langle\sigma^{(0)}_{ij}\right\rangle=\langle\rho\rangle\frac{\partial^2u^{(0)}_i}{\partial t^2} \tag{13}$$

where the macroscopic stress $\langle\sigma^{(0)}_{ij}\rangle\equiv\sum^{(0)}_{ij}$ is expressed as

$$\Sigma^{(0)}_{ij}=C_{ijkl}(d)e_{xkl}\left(\mathbf{u}^{(0)}\right) \tag{14}$$

where

$$C_{ijkl}(d)=\frac{1}{|Y|}\int_{Y_s}\left(a_{ijkl}+a_{ijmn}e_{ymn}\left(\xi^{kl}\right)\right)dy \tag{15}$$

are the homogenized coefficients. $\xi^{pq}(\mathbf{y})$ are the displacement fields in the unit cell problem for particular macroscopic deformations $e_{xpq}(\mathbf{u}^{(0)})$. $|Y|$ is the measure of Y and Y_s is the unit cell minus the scaled crack ($Y_s=Y/CY$).

The effective coefficients C_{ijkl} depends on the state of damage and the elastic properties of the solid matrix (E and ν). The coefficients C_{ijkl} defined by Eq. (15) can be computed by solving the unit cell problem for a large number of $d\in[0,1]$ assuming periodic boundary conditions. This aspect will be addressed in Section 3.2.

2.3. Damage evolution from energy release rate analysis

In this section, the more complex problem of evolving micro-cracks is considered, extending the homogenization method in order to obtain macroscopic evolution law for damage.

Under a given loading of the macroscopic structure, the resulting local state of stress leads to the activation of particular families of micro-cracks. In what follows, in such a macroscopic point, it is assumed that in a small vicinity a family of straight micro-cracks is activated and they are propagating in mode I, symmetrically with respect to their middle-point. For simplicity, we assume vertical micro-cracks even if the present framework can be extended to other crack orientations, as done in François and Dascalu (2010) under quasi-static conditions.

A Griffith-type energy criterion is considered: propagation occurs when a critical energy threshold $\mathscr{G}_c$ is reached. The crack propagation is described by the following relations:

$$\mathscr{G}^{d\varepsilon}\le\mathscr{G}_c;\quad \frac{dl}{dt}\ge 0;\quad \frac{dl}{dt}\left(\mathscr{G}^{d\varepsilon}-\mathscr{G}_c\right)=0 \tag{16}$$

where $\mathscr{G}_c$ is the critical fracture energy of the material and $\mathscr{G}^{d\varepsilon}$ is the energy release rate in dynamics at the crack tip.

On one hand, Keita et al. (2014) demonstrated that, during crack propagation, the energy release rate in dynamics can be expressed as a function of microscopic variables:

$$\mathscr{G}^{d\varepsilon}=\mathscr{G}^{\varepsilon}+\varepsilon\frac{1}{2}\rho c_p^2\lim_{r\to 0}\int_{\Gamma Y_r}\left(\frac{\partial\mathbf{u}^{(1)}}{\partial y_2}\right)^2n_2ds_y \tag{17}$$

where $\mathscr{G}^{\varepsilon}=\varepsilon\mathscr{G}_y$, $\mathscr{G}_y$ being the energy release rate in the unit cell problem. Here ΓY_r is a circle of an infinitesimal radius r surrounding the crack tip in the unit cell problem and n_2 is the y_2-component (in the direction of the crack propagation) of the unit normal vector on ΓY_r (see Fig. 2). c_p is the speed of crack propagation.

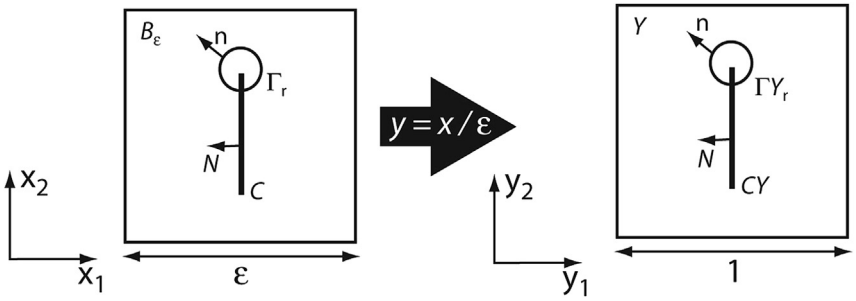

Fig. 2. Rescaling of the unit cell to the microstructural period of the material. $\mathscr{B}_\varepsilon$ is the full domain with $\mathscr{C}$ the union of all micro-cracks inside $\mathscr{B}$. Y is the unit cell with CY the scaled crack.

On the other hand, for the tensile crack growth at nonuniform speed, the physical energy release rate in dynamics is expressed as a function of the stress intensity factor in mode I as follows (Freund, 1998):

$$\mathscr{G}^{d\varepsilon} = \frac{1-\nu^2}{E}\left(K_I^{\varepsilon}\right)^2 - \frac{\dot{l}}{C_R}\frac{1-\nu^2}{E}\left(K_I^{\varepsilon}\right)^2 \tag{18}$$

where K_I^{ε} represents the static stress intensity factor in mode I and C_R is the Rayleigh waves speed:

$$C_R = \frac{0.862+1.14\nu}{1+\nu}\sqrt{\frac{E}{2\rho(1+\nu)}} \tag{19}$$

Comparing Eq. (17) to Eq. (18) the following equalities can be identified

$$\mathscr{G}^{\varepsilon} = \frac{1-\nu^2}{E}\left(K_I^{\varepsilon}\right)^2 \tag{20}$$

$$\varepsilon\frac{1}{2}\rho c^2 \lim_{r\to 0}\int_{\Gamma_r}\left(\frac{\partial \mathbf{u}^{(1)}}{\partial y_1}\right)^2 n_1 ds_y = -\frac{\dot{l}}{C_R}\frac{1-\nu^2}{E}\left(K_I^{\varepsilon}\right)^2 \tag{21}$$

Eq. (20) represents the classical relation between the energy release rate and the stress intensity factor in mode I under quasi-static conditions while Eq. (21) is the dynamic corrector due to the inertial effect (i.e. the micro-crack propagation speed is limited by the Raleigh waves velocity).

As detailed in Keita et al. (2014), the macroscopic damage equation in dynamics can be obtained through the generalisation of the quasi-static case developed in Dascalu et al. (2008) for brittle micro-fracture by substituting the quasi-static energy release rate by the energy release rate in dynamics.

In Dascalu et al. (2008) the following relation was deduced, based on quasi static evolution of microcracks:

$$\frac{dd}{dt}\left(\frac{1}{2}\frac{\partial C_{ijkl}(d)}{\partial d}e_{xkl}\left(\mathbf{u}^{(0)}\right)e_{xij}\left(\mathbf{u}^{(0)}\right) + \mathscr{G}_y\right) = 0 \tag{22}$$

This relation still holds in our case if $\mathscr{G}_y$ represents the energy release rate in the unit cell problem calculated with the dynamic corrector.

By replacing $\mathscr{G}_y$ by $\mathscr{G}^{d\varepsilon}$ expressed as a combination of Eqs. (16), (17), (20) and (21), Keita et al. (2014) established the following equation

$$\frac{dd}{dt}\left(\frac{1}{2}\frac{\partial C_{ijkl}(d)}{\partial d}e_{xkl}\left(\mathbf{u}^{(0)}\right)e_{xij}\left(\mathbf{u}^{(0)}\right) + \frac{\mathscr{G}_c}{\varepsilon}\left(1+\frac{\varepsilon\dot{d}}{C_R-\varepsilon\dot{d}}\right)\right) = 0 \tag{23}$$

that can be re-written for evolving damage (i.e. when $dd/dt \neq 0$) in the form

$$\frac{dd}{dt} = \frac{2C_R}{\varepsilon}\left(\frac{\mathscr{G}_c}{\varepsilon\frac{\partial C_{ijkl}(d)}{\partial d}e_{xkl}\left(\mathbf{u}^{(0)}\right)e_{xij}\left(\mathbf{u}^{(0)}\right)} + \frac{1}{2}\right) \tag{24}$$

as the dynamic damage evolution law.

Upon micro-crack propagation, the quasi-static damage equation represents the limit case of the dynamic damage equation when $\frac{\dot{l}}{C_R} \ll 1$. This means that when the crack propagation speed $\dot{l}$ is very small compared to the material Rayleigh waves speed C_R, the dynamic damage equation corresponds to the quasi-static case.

The internal length ε appears explicitly in the damage evolution Eq. (24) because this damage equation inherits the features of the micro-fracture laws (16) that represent a size-dependent model. So, this damage evolution law includes similar ingredients than the strain gradient constitutive models developed through homogenization schemes by Smyshlyaev and Cherednichenko (2000), Kouznetsova et al. (2002), Peerlings and Fleck (2004) or Tran et al. (2012).

3. Microscopically-based macroscopic model

3.1. Macroscopic problem

The macroscopic transient problem to be solved reduces to the homogenized momentum equilibrium equation in dynamics (13), the homogenized stress–strain relationship (14), the damage evolution law (24) and the damage irreversible condition ($dd/dt > 0$).

Under one-dimensional strain field (in the direction 1), as addressed in Section 5, this set of equations reduces to:

$$\frac{\partial \Sigma_{ij}^{(0)}}{\partial x_j} = \langle\rho\rangle\frac{\partial^2 u_1^{(0)}}{\partial t^2} \tag{25}$$

$$\Sigma_{ij}^{(0)} = C_{ij11}(d)e_{x11}\left(\mathbf{u}^{(0)}\right) \tag{26}$$

$$\frac{dd}{dt} = \frac{2C_R}{\varepsilon}\left(\frac{\mathscr{G}_c}{\varepsilon\frac{\partial C_{1111}(d)}{\partial d}e_{x11}\left(\mathbf{u}^{(0)}\right)e_{x11}\left(\mathbf{u}^{(0)}\right)} + \frac{1}{2}\right) \geq 0 \tag{27}$$

3.2. Homogenized stiffness coefficients

The homogenized coefficients C_{ijkl} can be computed numerically by applying the elementary modes of deformation on the unit cell with periodic conditions, for different values of damage variables between [0,1]. This has been done for the six modes of deformations (i.e. horizontal, vertical and shearing deformations, in crack-opening and crack-closure configurations) in Dascalu et al. (2008) for one specific set of Young modulus E and Poisson ratio ν. For the sake of simplicity, it is proposed here to linearize the evolution of the C_{ijkl} coefficients with respect to d. This is illustrated in Fig. 3 for the homogenized coefficients involved in the one-dimensional strain field problem in crack opening mode (C_{ij11}). The applicability of the obtained results below is by no means limited to this linearized evolution of the homogenized coefficients. The conclusions would remain valid for the real evolution of homogenized coefficients.

For intact material (i.e. for $d = 0$), the homogenized stiffness coefficients are equal to the elastic stiffness coefficient of the solid matrix. For the components concerned by the one-dimensional problem, it gives:

$$C_{1111,d=0} = a_{1111} = \frac{(1-\nu)E}{(1+\nu)(1-2\nu)} \tag{28}$$

$$C_{2211,d=0} = a_{2211} = \frac{\nu E}{(1+\nu)(1-2\nu)} \tag{29}$$

$$C_{1211,d=0} = C_{2111,d=0} = 0 \tag{30}$$

When the material is fully damaged, it is not able to transmit any tensile stress in the direction normal to the crack, leading to:

$$C_{1111,d=1} = C_{2211,d=1} = C_{1211,d=1} = C_{2111,d=1} = 0 \tag{31}$$

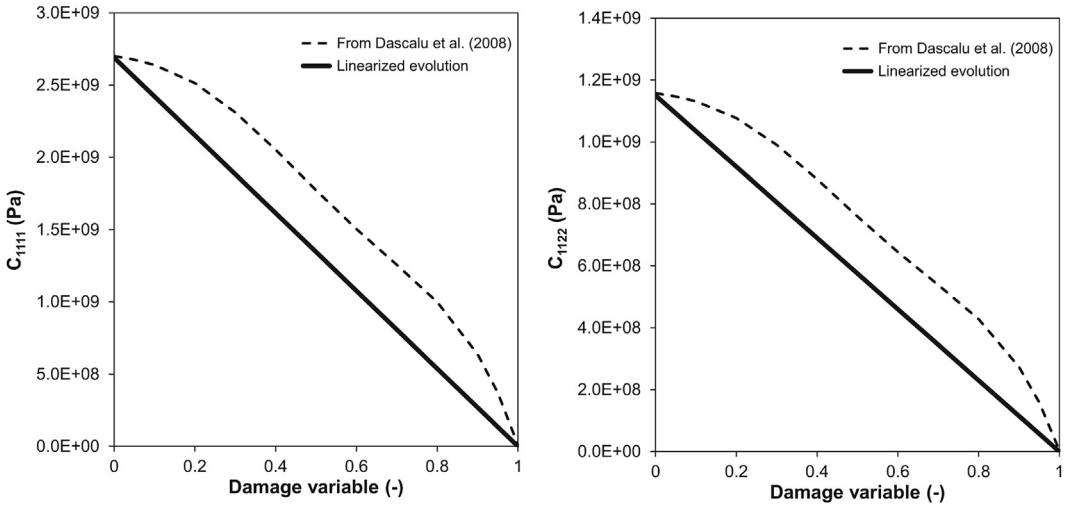

Fig. 3. Homogenized coefficients in crack opening mode (involved in the one-dimensional problem) as a function of damage for $E = 2.10^9\ Pa$ and $\nu = 0.3$. Comparison between real evolution (from Dascalu et al. (2008)) and the linearized evolution used in this study.

As presented in Fig. 3, between the intact stiffness for $d = 0$ and the vanishing stiffness for $d = 1$, the stiffness is assumed to evolve linearly.

$$C_{ij11}(d) = C_{ij11,d=0}(1-d) \tag{32}$$

3.3. Numerical algorithm

The dynamic damage model has been implemented in the LAGAMINE finite element code (Charlier, 1987) under two-dimensional plane strain configuration, the one-dimensional problem treated in this study being a particular application of this more general case. LAGAMINE offers an implicit time integration scheme to solve highly nonlinear transient problems in continuum mechanics in quasi-static or dynamic conditions. In the following, only the integration of the constitutive law is detailed.

In the constitutive subroutine, for each iteration and at each integration point, the input variables are the imposed strain state e_{x11}, the imposed strain rate $\dot{e}_{x11}$ and the damage variable d^i while the output variables are the stress state $\Sigma_{ij}^{(0)}$ and the updated damage variable d^{i+1} that are obtained according to the following steps:

1. The homogenized coefficients C_{ijkl} are obtained as a function of d^i.
2. The damage variation dd/dt is obtained from the damage evolution law (Eq. (24)) as a function of $C_{ijkl}(d^i)$ and e_{xij}
3. The damage variable is updated $d^{i+1} = d^i + \frac{dd}{dt}dt$
4. The homogenized coefficients C_{ijkl} are updated as a function of d^{i+1}
5. The stress state is obtained as $\sum_{ij}^{(0)} = C_{ijkl}e_{xkl}$

4. Rate-dependent local macroscopic response

The stress-strain macroscopic response is rate dependent due to the time-dependent damage evolution law (Eq. (24) in 3D and Eq. (27) under uniaxial strain condition). The Kuhn-Tucker criterion ($\frac{dd}{dt} \geq 0$) imposes that the damage does not evolve below a given strain level. Accordingly, when the damage energy release rate $\left|\frac{1}{2}\frac{\partial C_{1111}(d)}{\partial d}e_{x11}(\mathbf{u}^{(0)})e_{x11}(\mathbf{u}^{(0)})\right|$ is lower than the upscaled critical fracture energy $\mathcal{G}_c/\varepsilon$, the damage variable remains constant. This case corresponds to a negative damage evolution which is forbidden by the Kuhn-Tucker criterion. For higher strain level, the damage energy release rate overpasses the upscaled critical fracture energy and damage increases according to Eq. (27). The axial strain corresponding to the criterion of damage initiation can be easily obtained by equaling Eq. (27) to zero:

$$e_{x11,damage} = \sqrt{-\frac{2\mathcal{G}_c}{\varepsilon\frac{\partial C_{1111}(d)}{\partial d}}} \tag{33}$$

For extremely high damage energy release rate, the first term in the bracket of Eq. (27) becomes negligible and the speed of damage evolution is limited to C_R/ε. This is a consequence of the inertial effect at the crack tip.

Consequently, the internal length ε influences the strength of material (i.e. the criterion for the initiation of damage evolution) as well as the rate of this evolution.

To illustrate the paramount importance of ε, it is proposed in this section to simulate the local macroscopic response of material on two sets of simulations: tensile tests (i) at constant uniaxial strain and (ii) upon a uniaxial tensile strain ramp at constant strain rate.

Material parameters are reported in Table 1. All parameters are kept unchanged for all simulations excepted the internal length for which three different values are considered.

4.1. Constant uniaxial tensile strain

This series of simulations consists in tensile relaxation tests. The strain is maintained constant beyond the criterion of damage initiation. The loss of stiffness due to damage increase induces a progressive stress relaxation into the material. When the material is fully damaged, the stiffness, and by consequence the stress, vanishes. First, the effect of internal length is evaluated. An extreme tensile strain is applied. The obtained results are reported in Fig. 4 in terms of stress and damage evolution for the three considered internal length. As expected, it demonstrates that the time-

Table 1
Material parameters used in the simulations.

$E[Pa]$	$\nu[-]$	$G_c[J.m^{-2}]$	$\rho[kg/m]3$	$d_0[.]$	$\varepsilon[m]$
2.10^9	0.3	1.25	1912	0	$2.5.10^{-4}/1.10^{-3}/5.10^{-3}$

dependent response of the material depends on the microstructure. Upon very high strain, the velocity of crack propagation is limited by the speed of Raleigh waves. Consequently, starting from an undamaged material, full damage is obtained after a time corresponding to the size of the periodic cell divided by the Raleigh waves speed:

$$t_{damage}^{min} = \frac{\varepsilon}{C_R} \tag{34}$$

This can be understood intuitively because it is the time needed by the microcrack to reach the border of the periodic cell at a speed of Rayleigh waves. Also, it can be recovered through the damage evolution equation (27). When the strain is extremely high ($e_{x11} \gg$), the first term in the bracket vanishes and the rate of damage is C_R/ε.

In such a way, larger is the microstructure and more ductile is the material. The brittleness is limited by the time needed for the micro-crack to propagate until the border of the periodic cell.

Then, it is proposed to study the effect of the strain level for a given internal length. Fig. 5 reports the results for an internal length $\varepsilon = 1.10^{-3}\ m$ for five different strain levels, all of them being higher than the criterion for damage initiation. Actually, when the strain level decreases, the rate of damage propagation diminishes tending to zero (i.e. the time for full damage development tends to infinity) when the strain level reaches the strain corresponding to the criterion of damage initiation, called $e_{x11,damage}$ in Fig. 6.

4.2. Constant uniaxial tensile strain rate

A test with a constant increase of strain allows to exhibit all the phases of the material behaviour upon tension. First, before reaching the damage initiation criterion, the behaviour is purely elastic. Then,

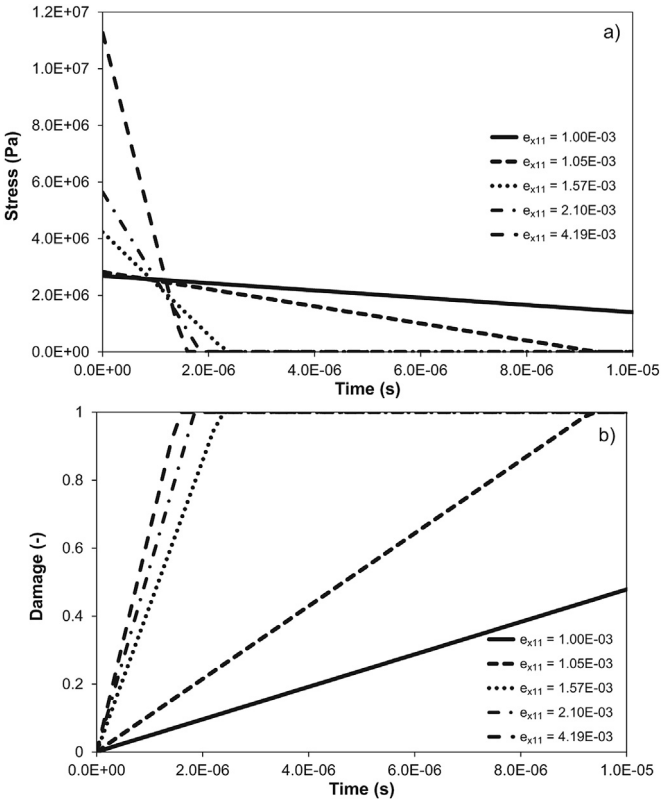

Fig. 5. Stress (a) and damage (b) evolution during relaxation tests upon different axial strain levels, for an internal length of $\varepsilon = 1.10^{-3}\ m$.

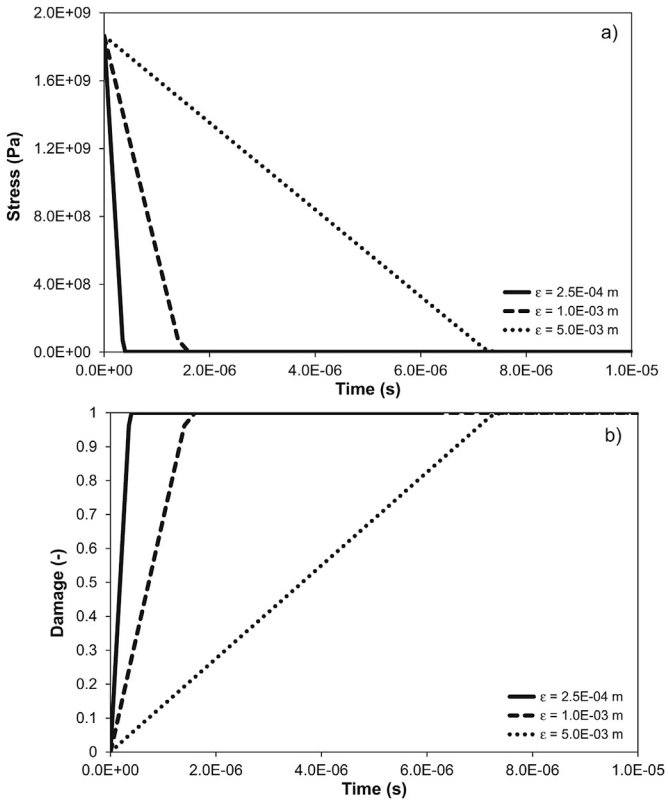

Fig. 4. Stress (a) and damage (b) evolution during relaxation tests upon very high axial strain ($e_{x11} = 0.2$), for different internal lengths ($\varepsilon = 2.5.10^{-4}\ m; 1.10^{-3}\ m; 5.10^{-3}\ m$).

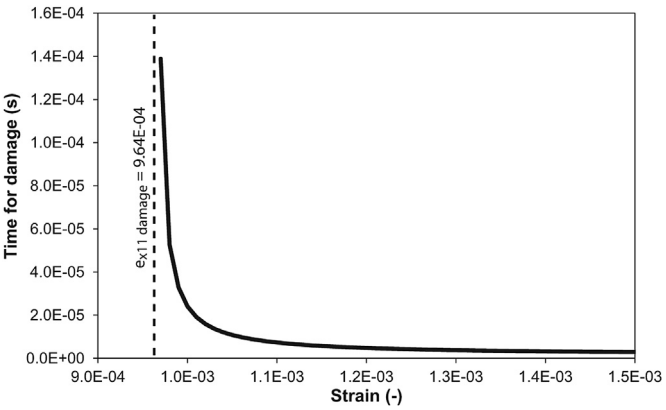

Fig. 6. Evolution of the time needed to reach a fully damaged material as a function of the level of constant tensile strain during a relaxation test.

when the strain goes over the damage initiation criterion, damage starts to increase, the secant stiffness decreases and the material reaches a peak of stress. When the peak is overpassed, the tangent stiffness becomes negative and the material experiences softening. This is illustrated in Fig. 7 for a strain rate of 125 s^{-1}. We clearly observe the effect of the internal length on the damage initiation criterion and the subsequent rate of damage increase.

The decrease of the micro-structure size ε produces an increase of the tensile strength together with an important reduction of ductility. On the one hand, the strength increase is explained by the activation of damage propagation criterion ($dd/dt > 0$) which depends on the micro-structure size ε (Eq. (27)).

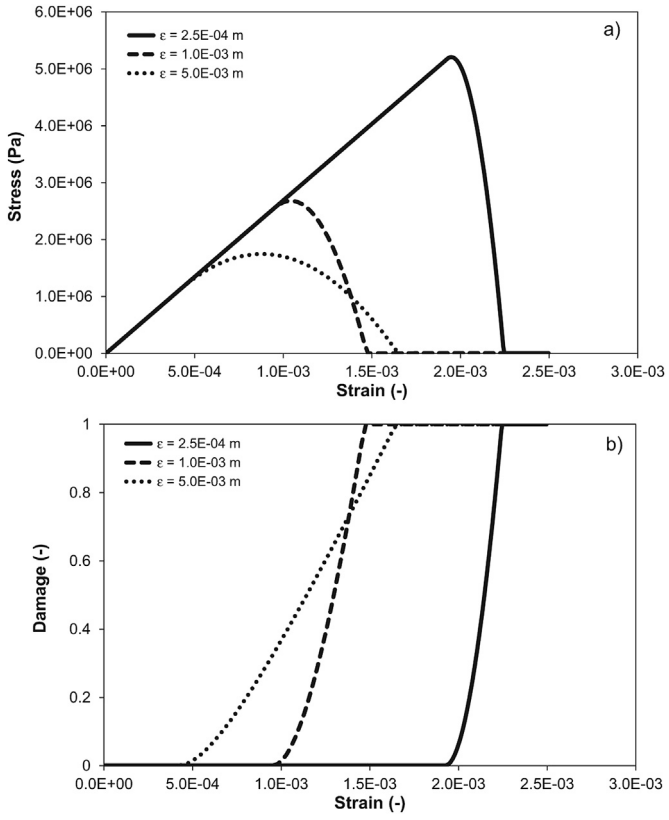

Fig. 7. Stress (a) and damage (b) evolution during tensile tests at a constant strain rate of 125 s^{-1} for three different internal lengths ($\varepsilon = 2.5.10^{-4}\ m; 1.10^{-3}\ m; 5.10^{-3}\ m$).

Following the energy criterion, larger cracks propagate easier than smaller ones. It expresses the Linear Elastic Fracture Mechanics size effect (Bazant, 2002) upscaled to damage at the macro-level. On the other hand, the decrease of ε leads to a more brittle macroscopic response because the crack reaches the border of the periodic cell faster for a smaller microstructure as already illustrated in Fig. 4. This effect is specific to dynamics since it depends on the rate dependent behavior of the crack propagation.

5. One-dimensional boundary value problem

5.1. Problem definition

In order to evaluate the ability of the model to regularize the process of strain localization in dynamics through the internal length, it is proposed to address the problem of a simple one-dimensional bar constrained laterally, fixed on one end and submitted to a sudden tensile stress on the other end (Fig. 8). This problem was previously addressed by Sluys and De Borst (1992) and Sluys et al. (1993). Earlier, Bazant and Belytschko (1985) and Belytschko et al. (1986) investigated similar case but the bar was free on both ends and equal and opposite velocities (or forces) were applied to the two ends of the bar.

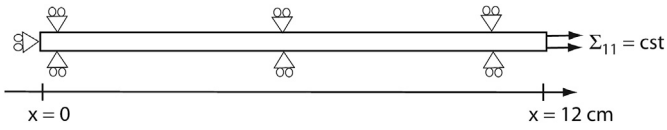

Fig. 8. Boundary conditions of the one-dimensional dynamic problem.

In both cases, strain softening is induced by the doubling of the tensile stress. For the case of the fixed bar on one end, loaded at the other end, the tensile wave reflects on the fixed end generating an additional tensile wave, leading to the doubling of the stress. In the case of the free bar loaded on both ends, the doubling of the stress takes place in the middle of the bar when the two waves meet each others. If this doubled stress overpasses the criterion for damage evolution, softening takes place.

In the present case, the bar has a length of 0.12 m and is divided into 100, 400 and 1000 elements, respectively. Eight-noded quadrilateral large strain finite elements with four Gauss points were used and the governing partial differential equations were solved with the Lagamine finite element code through a implicit Newmark's integration scheme with Newmark's parameters γ and β respectively equal to 0.8 and 0.4. A constant time step of $2.5.10^{-8}\ s$ has been taken.

Material parameters reported in Table 1 are still used in this case. In order to initiate damage when the stress is doubled after reflection, the magnitude of the impact load must be included between 50% and 100% of the axial stress corresponding to the criterion of damage initiation (called the damage stress in what follows). According to Eq. (33), this damage stress is

$$\sum_{11,damage} = C_{1111} e_{x11,damage} = C_{1111}\sqrt{\frac{1}{2}\frac{\mathscr{G}_c}{\varepsilon \frac{\partial C_{1111}(d)}{\partial d}}} \tag{35}$$

The magnitude of impact tensile load has been taken equal to $0.75 \times \Sigma_{11,damage}$. However, the specificity of the present damage evolution law is that the criterion for damage initiation depends on the internal length, as observed in Eq. (35) and discussed in Section 4.2. So, the magnitude of impact load has been adapted for each internal length, as reported in Table 2.

5.2. Internal length as a regulation variable

Fig. 9 presents, first, the purely elastic problem when the applied impact load is not high enough to generate damage evolution after the doubling of the tensile stress. In this case, the applied stress was equal to $1.10^5\ Pa$. The elastic wave propagates at a speed of $c_e = \sqrt{\frac{C_{1111}}{\rho}} = 1186 m/s$ leading to a travel time of $1.01.10^{-4}\ s$ (needed to obtain the reflection of the wave at the fixed end). After reflection at $x = 0$, the reflected wave is added to the incidental wave leading to a doubling of the stress.

Fig. 10 presents the stress profile induced by the applied load corresponding to $0.75 \times \Sigma_{11,damage}$ for the intermediate mesh size (400 elements) and an internal length of $1.10^{-3}\ m$. As expected, the doubling of the stress due to wave reflection produces damage at the end of the bar. Actually, when the material is fully damaged, the stiffness is reduced to zero and the fixed boundary condition is transformed into a free boundary condition. Consequently, the tensile wave is then reflected into a compression wave and the incidental and reflected waves cancel each other.

Damage profile in the bar at different times in the vicinity of the fixed end is illustrated in Fig. 11 together with the evolution

Table 2
Magnitude of applied tensile load taken as 75% of the damage stress depending on the internal length.

$\varepsilon[m]$	$2.5.10^{-4}$	1.10^{-3}	5.10^{-3}
$\Sigma_{11,damage}[Pa]$	$5.2.10^6$	$2.6.10^6$	$1.16.10^6$
$\Sigma_{11,applied}[Pa]$	$3.9.10^6$	$1.95.10^6$	$0.87.10^6$

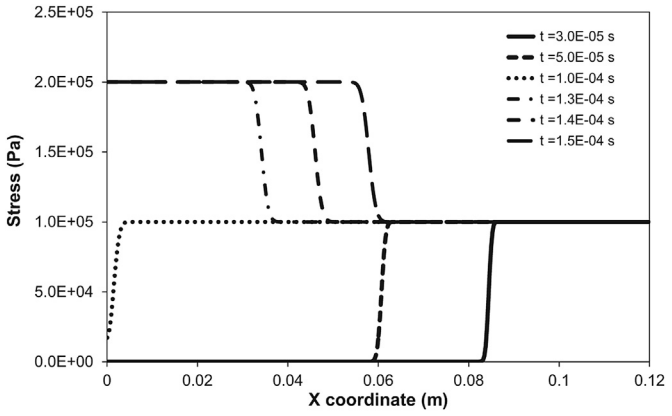

Fig. 9. Stress profile during elastic wave propagation, obtained with a regular mesh of 400 elements. The impact is applied at $x = 0.12$ m. The wave propagates through the material and is reflected on the fixed end (at $x = 0$ m.).

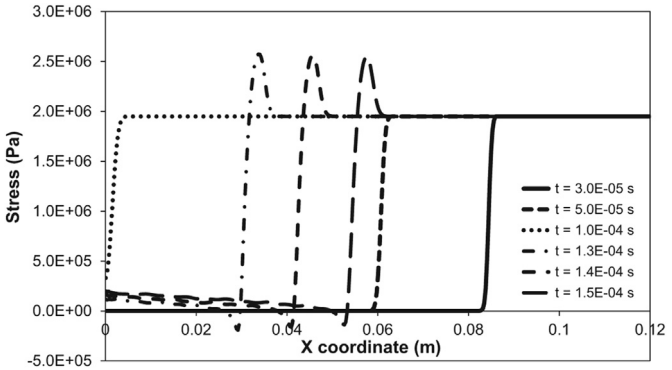

Fig. 10. Stress profile at different times for an applied load of $0.75 \times \Sigma_{11,damage}$ and an internal length $\varepsilon = 1.10^{-3}$ m, obtained with a regular mesh of 400 elements.

of the tensile stress profile, for an internal length of $\varepsilon = 1.10^{-3}$ m. Attention is mainly focused on times corresponding to the period of damage development: from the wave reflection to the moment when the thickness of the band is fully developed. When the front of the incidental wave reaches the fixed end, the reflected wave sums up with the incidental one and the stress progressively increases. When the magnitude of the tensile stress reaches the damage stress, damage increases, stiffness decreases and consequently the stress progressively drops. When the damage is fully developed in a given zone, the stress vanishes in that zone and produces an impenetrable barrier for the wave. So, the subsequent reflection takes place in the form of a compression wave that cancels the incidental tensile wave. Stress vanishes progressively in the entire bar and no more damage can be generated.

Fig. 12 follows the stress–strain relationship of the material at different locations in the damaged zone. Points located in the fully damaged zone, close to the end of the bar, are submitted to a monotonic strain loading leading to a peak response followed by a stress decrease due to the softening process. On the contrary, strains in the partially damaged zone vanish after the peak. Actually, the strain is localized in the fully damaged zone while out of that zone the material is unloaded due to the reflected compression wave. Conceptually, as long as the damage variable is lower than one, the material is able to transmit the wave and the strain returns to zero when the tensile stress is canceled by the reflected compressive stress. When damage variable reaches one, stiffness vanishes and the strain tends

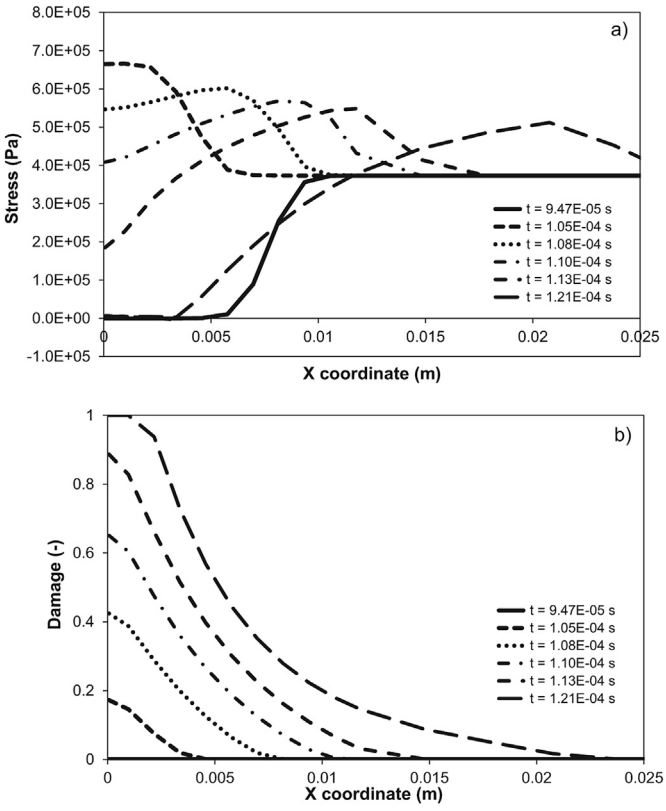

Fig. 11. (a) Stress and (b) damage profile in the vicinity of the fixed end of the bar (zoom on the 2.5 cm close to the fixed end) at different times during the development of the localized damaged band for $\varepsilon = 1.10^{-3}$ m, obtained with a regular mesh of 400 elements.

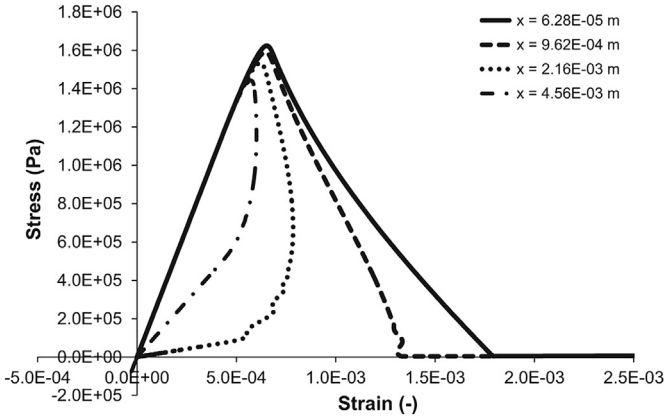

Fig. 12. Stress-strain behaviour at different locations in the localized damaged zone for $\varepsilon = 1.10^{-3}$ m, obtained with a regular mesh of 400 elements.

theoretically to infinity. In practice, a residual stiffness 1000 times smaller than intact stiffness is imposed to avoid the stop of the computation.

In the fully damaged zone, the post-peak stress-strain curves show a brittleness that increases when the distance to the left boundary increases. This is due to the rate-dependent response of the model, for which strength and ductility increase with the strain rate. In the studied boundary value problem, the strain rate is higher, closer to the fixed boundary. This is because the incidental wave and the reflected wave interact in a very short period of time close to the boundary. Consequently, it generates rapid

changes of stress and strain close to the boundary, leading to high strain rate.

So, the damage is spread out over time and the drop of material stiffness is progressive. Consequently, the contrast of the mechanical impedance between damaged and undamaged zones is smooth. A part of the wave can still propagate in the zone which is under on-going damage in order to reach further region and increases the thickness of damaged zone.

By opposition, if the softening process was immediate, the stiffness would vanish in the first element, that would lead to an intense straining in that element. The result would be mesh-sensitive in the sense that the strain localization would take place on a thickness of one element, the smallest possible zone. In other words, instantaneous softening would provide an impenetrable barrier for the wave. Consequently, the wave could not propagate further in the material to increase the thickness of the strain localisation band.

Most importantly, Fig. 13 demonstrates that the strain localization is mesh-independent. The thickness of the localized zone converges to a finite value. For the coarser mesh, the results slightly deviate for the smallest microstructure because the "physical" thickness of the localized band is close to the size of the elements. It is also shown that the thickness of the band is governed by the internal length. This will be discussed in the next section.

6. Discussions

As discussed previously, the introduction of an internal length in a strain softening model to make the problem of strain localization well-posed is not new. Needleman (1988) has shown that a rate-dependent model implicitly introduces a characteristic length $l_{charact}$ that can be considered as the distance an elastic wave travels at a speed c_e in a characteristic time $t_{charact}$ (Sluys and De Borst, 1992):

$$l_{charact} = c_e t_{charact} \tag{36}$$

The characteristic time $t_{charact}$ is the time needed for the softening to be fully developed. In other words, time-dependence induces a delay in the loss of material stiffness which, in turn, when multiplied by the velocity of wave propagation, results in a characteristic length. This length controls the thickness of the localized band.

The present approach can be seen as the reversal of the concept introduced by Needleman (1988). We start from an internal length ε which is the natural microstructural size of the material. The rate-dependent response of the material follows from this internal length because the micro-crack needs a given time to propagate until the border of the periodic cell. This inertial effect is based on an energy analysis at the crack tips stating that the upper limit of the speed of crack propagation is the speed of Raleigh waves. In the limit case of an extreme loading, using Eq. (34), our characteristic length is

$$l_{charact} = c_e t_{charact} = c_e \frac{\varepsilon}{C_R} \tag{37}$$

For a Poisson ratio equal to 0.3, it gives $l_{charact} = 1.97\varepsilon$. Actually, this coefficient close to two is related to the fact that elastic wave propagates as a P-wave (under a speed $c_e = V_p$) while the crack speed is controlled by the Raleigh wave speed (C_R). For $\nu = 0.3$, V_p is approximately twice bigger than C_R. In other words, the crack propagates through the periodic cell from the center to the border of the cell in the same time than the wave crosses two periodic cells. For other values of ν, the ratio between characteristic and internal lengths would be different.

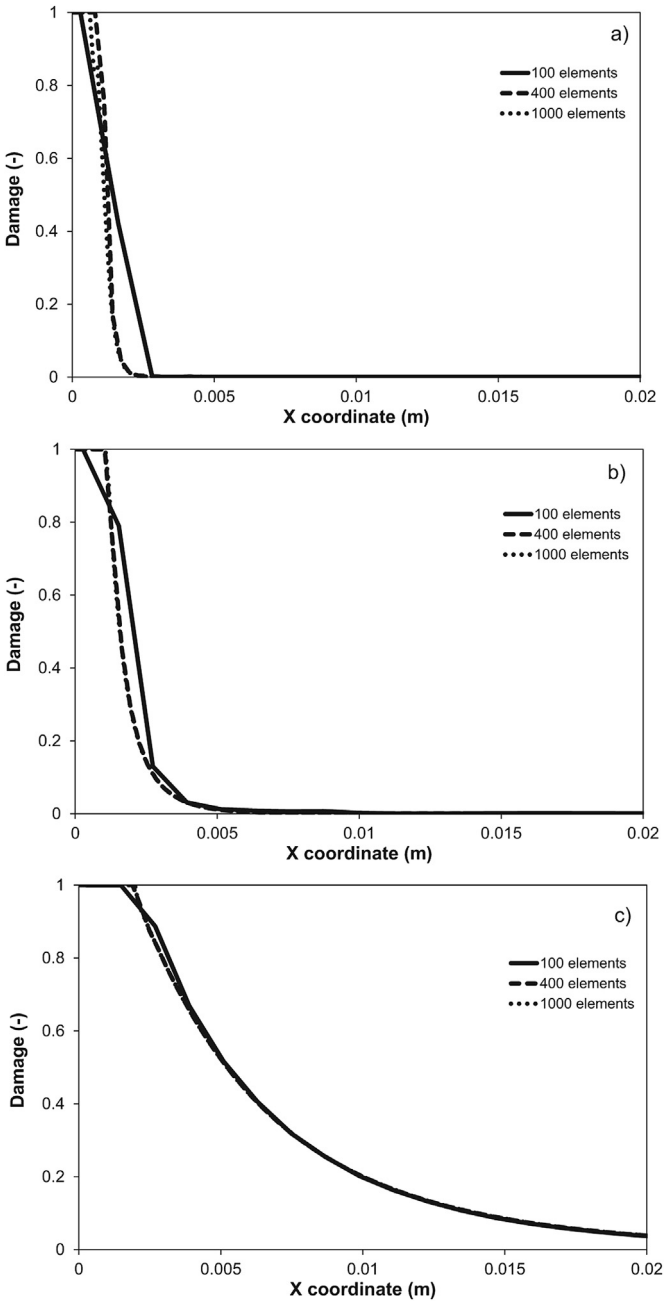

Fig. 13. Localized damage at the fixed end of the bar independent of the mesh size, for three internal lengths: (a) $\varepsilon = 2.5.10^{-4}\ m$; (b) $\varepsilon = 1.10^{-3}\ m$; (c) $\varepsilon = 5.10^{-3}\ m$. Zoom on the 2 cm close to the fixed end).

Actually, the thickness of the band is not exactly equal to the characteristic length as defined in Eq. (37) mainly for two reasons. First, the speed of crack propagation is always lower than the speed of Rayleigh waves; the speed of Rayleigh wave being the upper limit under extremely high loading. Secondly, under damage evolution, the material stiffness gradually decreases and, consequently, the speed of wave propagation also decreases. However, the characteristic length, as computed by Eq. (37) gives a first estimation of the expected thickness of localized band.

7. Conclusions

Mechanical boundary value problems considering material softening suffers from pathological mesh-dependence response for

classical rate-independent constitutive laws. Various techniques are available to regularize the problem and to remove the mesh sensitivity of the solution. The main concept is to introduce, directly or indirectly, a characteristic length in the material that control the thickness of the band. It is supposed that this length depends on the material microstructure. However, when phenomenological models are used, this length is often a calibration parameter which is not really microstructurally based.

The starting point of the present model is the periodically cracked microstructure, that includes intrinsically an internal length (i.e. the distance between two adjacent micro-cracks). This internal length that regularizes the strain localization problem is directly taken as the size of the microstructure. From a conceptual point of view, it is a major advantage because the thickness of the strain localization is only function of quantifiable parameters (i.e. the speed of the stress wave and the size of the microstructure). However, if the size of the microstructure is not available from direct measurements, the internal length remains a material parameter that can still be calibrated to fit macroscopic results.

From this idealized microstructure, a rate-dependent damage evolution law is constructed by asymptotic homogenization and energy analysis at the crack tips. Consequently, inertial effect is considered because the speed of crack propagation is limited by the speed of Raleigh waves. The induced damage is not immediate but depends on the velocity of micro-crack propagation and the size of the periodic cell.

The delay in the induced damage provides ductility to the material. The drop of material stiffness is spread out over time. Consequently, the wave that induces the damage is not immediately reflected on the damaged zone but may penetrate in further regions in order to induce damage propagation on a given thickness. This case has been illustrated in a one-dimensional problem for which, we have shown that the strain localization phenomenon develops on a finite thickness which is mesh-insensitive.

So, we have demonstrated, through a simple boundary value problem, that the periodicity of the microstructure controls the thickness of the damaged zone in a dynamic problem. The considered microstructure (a single cracked cell) has the merits of simplicity and allows applying the concept of dynamic fracture mechanics at the scale of the microstructure. However, it is clear that in reality, the distribution patterns of micro-cracks may be more complex. In particular, the density of cracks may increase in the damaged zone, reducing the inter-distance between cracks. This would require additional developments to be considered in this general framework.

References

Aifantis, E.C., 1984. On the microstructural origin of certain inelastic models. J. Eng. Mater. Technol. 106 (4), 326–330.

Ashby, M.F., Hallam, S.D., 1986. The failure of brittle solids containing small cracks under compressive stress states. Acta Metall. 34, 497–510.

Bhatt, H., Rosakis, A., Sammis, G., 2011. A micro-mechanics based constitutive model for brittle failure at high strain rates. J. Appl. Mech. 79 (3), 1016–1028.

Bazant, Z.P., Belytschko, T., Chang, T., 1984. Continuum theory for strain softening. J. Eng. Mech. 110 (12), 1666–1692.

Bazant, Z.P., 1976. Instability, ductility, and size effect in strain-softening concrete. J. Eng. Mech. Div. 102 (2), 331–344.

Bazant, Z.P., 2002. Scaling of Structural Strength. Hermes Penton Science, London.

Bazant, Z.P., Belytschko, T.B., 1985. Wave propagation in a strain-softening bar : exact solution. ASCE J. Eng. Mech. 111 (3), 381–389.

Bazant, Z.P., Pijaudier-Cabot, G., 1998. Nonlocal continuum damage, localization instability and convergence. J. Appl. Mech. ASME 55, 287–294.

Belytschko, T., Bazant, Z.P., Hyun, Y.W., Chang, T.P., 1986. Strain-softening materials and finite-element solutions. Comput. Struct. 23 (2), 163–180.

Benssousan, A., Lions, J., Papanicolaou, G., 1978. Asymptotic Analysis for Periodic Structures. Kluwer Academic Publisher, Amsterdam.

Brace, W.F., Bombolakis, E.G., 1963. A note on brittle crack growth in compression. J. Geophys. Res. 68, 3709–3713.

Chambon, R., Caillerie, D., Matsushima, T., 2001. Plastic continuum with microstructure, local second gradient theories for geomaterials: localization studies. Int. J. Solids Struct. 38, 8503–8527.

Charlier, R., 1987. Approche unifiée de quelques problèmes non linéaires de mécanique des milieux continus par la méthode des éléments finis. PhD Thesis. Université de Liège.

Collin, F., Chambon, R., Charlier, R., 2006. A finite element method for poro mechanical modelling of geotechnical problems using local second gradient models. Int. J. Numer. Method Eng. 65, 1749–1772.

Dascalu, C., Bilbie, G., Agiasofitou, E., 2008. Damage and size effect in elastic solids:A homogenization approach. Int. J. Solid Struct. 45, 409–430.

De Borst, R., Sluys, L.J., 1991. Localisation in a Cosserat continuum under static and dynamic loading conditions. Comput. Methods Appl. Mech. Eng. 90 (1), 805–827.

De Borst, R., Sluys, L.J., Muhlhaus, H.B., Pamin, J., 1993. Fundamental issues in finite element analyses of localization of deformation. Eng. Comput. 10 (2), 99–121.

Desmorat, R., Chambart, M., Gatuingt, F., Guilbaud, D., 2010. Delay-active damage versus non-local enhancement for anisotropic damage dynamics computations with alternated loading. Eng. Fract. Mech. 77 (12), 2294–2315.

François, B., Dascalu, C., 2010. A two-scale time-dependent damage model based on non-planar growth of micro-cracks. J. Mech. Phys. Solids 58 (11), 1928–1946.

Freund, L.B., 1998. Dynamic Fracture Mechanics. Cambridge University Press.

Glema, A., Lodygowski, T., Perzyna, P., 2000. Interaction of deformation waves and localization phenomena in inelastic solids. Comput. Methods Appl. Mech. Eng. 183, 123–140.

Graff, S., Forest, S., Strudel, J.L., Prioul, C., Pilvin, P., Béchade, J.L., 2004. Strain localization phenomena associated with static and dynamic strain ageing in notched specimens: experiments and finite element simulations. Mater. Sci. Eng. A 387, 181–185.

Hill, R., 1962. Acceleration waves in solids. J. Mech. Phys. Solids 10 (1), 1–16.

Huang, C., Subhash, G., Vitton, S.J., 2002. A dynamic damage growth model for uniaxial compressive response of rock aggregates. Mech. Mater. 34, 267–277.

Keita, O., Dascalu, C., François, B., 2014. A two-scale model for dynamic damage evolution. J. Mech. Phys. Solids 64, 170–183.

Kouznetsova, V., Geers, M.G.D., Brekelmans, W.A.M., 2002. Multi-scale constitutive modelling of heterogeneous materials with a gradient-enhanced computational homogenization scheme. Int. J. Numer. Methods Eng. 54, 1235–1260.

Lasry, D., Belytschko, T., 1988. Localization limiters in transient problems. Int. J. Solids Struct. 24 (6), 581–597.

Mindlin, R., 1965. Second gradient of strain and surface-tension in linear elasticity. Int. J. Solids Struct. 1, 417–438.

Mühlhaus, H.B., 1989. Application of Cosserat theory in numerical solutions of limit load problems. Arch. Appl. Mech. 59 (2), 124–137.

Mühlhaus, H.B., Aifantis, E.C., 1991. A variational principle for gradient plasticity. Int. J. Solids Struct. 28, 845–858.

Needleman, A., 1988. Material rate dependance and mesh sensitivity in localization problems. Comput. Meth. Appl. Mech. Eng. 67, 69–85.

Nemat-Nasser, S., Horii, M., 1982. Compression-induced nonplanar crack extension with application to splitting, exfoliation, and rockburst. J. Geophys. Res. 87, 6805–7682.

Nemat-Nasser, S., Deng, H., 1994. Strain-rate effect on brittle failure in compression. Acta Metall. Mater. 42, 1013–1024.

Nicot, F., Darve, F., 2011. Diffuse and localized failure modes: two competing mechanisms. Int. J. Numer. Anal. Meth. Geomech. 35 (5), 586–601.

Pedersen, R.R., Simone, A., Sluys, L.J., 2008. An analysis of dynamic fracture in concrete with a continuum visco-elastic visco-plastic damage model. Eng. Fract. Mech. 75 (13), 3782–3805.

Peerlings, R.H.J., De Borst, R., Brekelmans, W.A.M., de Vree, J.H.P., 1996. Gradient enhanced damage for quasi-brittle materials. Int. J. Numer. Meth. Eng. 39, 937–953.

Peerlings, R.H.J., De Borst, R., Brekelmans, W.A.M., Geers, M.G.D., 2002. Localisation issues in local and nonlocal continuum approaches to fracture. Eur. J. Mech. A/Solids 21 (2), 175–189.

Peerlings, R.H.J., Fleck, N.A., 2004. Computational evaluation of strain gradient elasticity constants. Int. J. Multiscale Comput. Eng. 2, 599–619.

Pijaudier-Cabot, G., Bazant, Z.P., 1987. Nonlocal damage theory. J. Eng. Mech. 113 (10), 1512–1533.

Ravichandran, G., Subhash, G., 1995. A micromechanical model for high strain rate behavior of ceramics. Int. J. Solids Struct. 32, 2627–2646.

Sanchez-Palencia, E., 1980. Non-homogeneous Media and Vibration Theory. Lecture Notes in Physics, vol. 127. Springer, Berlin.

Smyshlyaev, V.P., Cherednichenko, K.D., 2000. On rigorous derivation of strain gradient effects in the overall behaviour of periodic heterogeneous media. J. Mech. Phys. Solids 48, 1325–1357.

Sluys, L.J., De Borst, R., 1992. Wave propagation and localization in a rate-dependent cracked medium–model formulation and one-dimensional examples. Int. J. Solids Struct. 29 (23), 2945–2958.

Sluys, L.J., De Borst, R., Mühlhaus, H.-B., 1993. Wave propagation, localization and dispersion in a gradient-dependent medium. Int. J. Solids Struct. 30 (9), 1153–1171.

Sulem, J., 2010. Bifurcation theory and localization phenomena. Eur. J. Environ. Civ. Eng. 14 (8–9), 989–1009.

Tran, T.-H., Monchiet, V., Bonnet, G., 2012. A micromechanics-based approach for the derivation of constitutive elastic coefficients of strain-gradient media. Int. J. Solids Struct. 49, 783–792.

Wang, W.M., Sluys, L.J., De Borst, R., 1996. Interaction between material length scale and imperfection size for localization phenomena in viscoplastic media. Eur. J. Mech. A/Solids 15, 447–464.
Wang, E.Z., Shrive, N.G., 1995. Brittle fracture in compression: mechanisms, models and criteria. Eng. Fract. Mech. 52, 1107–1126.
Wong, T.F., 1990. A note on the propagation behaviour of a crack nucleated by a dislocation pile-up. J. Geophys. Res. 95, 8639–8646.
Wu, F.H., Freund, L.B., 1984. Deformation trapping due to thermoplastic instability in one-dimensional wave propagation. J. Mech. Phys. Solids 32 (2), 119–132.
Zhang, J.X., Wong, T.F., Davis, D.M., 1990. Micromechanics of pressured-induced grain crushing in porous rocks. J. Geophys. Res. 95, 341–351.